Submitted to Materials Science
and Engineering

UCRL-20554
Preprint

c.2

HIGH VOLTAGE ELECTRON MICROSCOPY STUDIES OF PHASE TRANSFORMATIONS IN COBALT FERRITES

Lutgard C. De Jonghe and G. Thomas

May 1971

AEC Contract No. W-7405-eng-48

TWO-WEEK LOAN COPY

This is a Library Circulating Copy
which may be borrowed for two weeks.
For a personal retention copy, call
Tech. Info. Division, Ext. 5545

UCRL-20554

LAWRENCE RADIATION LABORATORY
UNIVERSITY of CALIFORNIA BERKELEY

DISCLAIMER

This document was prepared as an account of work sponsored by the United States Government. While this document is believed to contain correct information, neither the United States Government nor any agency thereof, nor the Regents of the University of California, nor any of their employees, makes any warranty, express or implied, or assumes any legal responsibility for the accuracy, completeness, or usefulness of any information, apparatus, product, or process disclosed, or represents that its use would not infringe privately owned rights. Reference herein to any specific commercial product, process, or service by its trade name, trademark, manufacturer, or otherwise, does not necessarily constitute or imply its endorsement, recommendation, or favoring by the United States Government or any agency thereof, or the Regents of the University of California. The views and opinions of authors expressed herein do not necessarily state or reflect those of the United States Government or any agency thereof or the Regents of the University of California.

HIGH VOLTAGE ELECTRON MICROSCOPY STUDIES OF PHASE TRANSFORMATIONS IN COBALT FERRITES

Lutgard C. De Jonghe* and G. Thomas

Inorganic Materials Research Division, Lawrence Radiation Laboratory
Department of Materials Science and Engineering, College of Engineering
University of California, Berkeley, California

ABSTRACT

Phase transformations in the reducing atmosphere of the electron microscope have been examined in detail. It has been shown that these transformations are due to the loss of oxygen from the specimen surface. A time dependent gradient in the cation/anion ratio is developed from the surface of the transforming foil, and initially cobalt metal, containing less than 5 at% iron, has been found to form at the specimen surface. At the same time a very high density of small (30-40Å) cobalt-wüstite particles precipitates within the foil. This (Co,Fe)O phase probably forms homogeneously. After prolonged heating, the specimen is converted to a mixture of cobalt (fcc and hcp) metal grains, and an iron rich spinel matrix.

Studies of transformations in air have shown that (Co,Fe)O precipitates initially are shaped as square prisms, and are fully coherent up to a size of at least 1200Å. Between 1200 and 1500Å they lose coherency, and also become more or less spherical in shape. Undissociated interface dislocations are then resolved. During growth, micropores were found to migrate along with the semicoherent interfaces. Their origin and a possible mechanism by which precipitates lose coherency is discussed.

* Now at the Gordon McKay Laboratory, Harvard University, Cambridge, Mass.

I. INTRODUCTION

During the past fifteen years, electron microscopy has proved its unique usefulness in establishing the relation between microstructure and mechanical properties of metals and alloys. For the examination of ceramic materials, however, the transmission electron microscope is not yet a standard tool, since most practical ceramics have a very complex multiphase structure from which electron transparent foils are difficult to prepare. With the commercial introduction of high voltage microscopes, and the continued development of foil preparation techniques, such as ion bombardment, these experimental difficutlies are no longer obstacles to the substructural characterization of ceramics. Such an approach is necessary, particularly with regard to phase transformations in systems such as metal oxides, if the mechanical, electrical and magnetic properties of ceramics are to be understood and developed.

In this paper phase transformations in cobalt ferrite single crystals have been investigated. This cubic oxide has been selected for a number of reasons: Cobalt ferrites have the spinel structure, and currently about thirty different cations are known to form spinels with oxygen.[1] It is hoped that some of the information about cobalt ferrites obtained here would be relevant to this large class of crystals. Also, this ferrite, like several others, is ferrimagnetic, and for this reason has found applications in electronics industries.[2] Conventionally, grain size or porosity has been used to control the magnetic properties of polycrystalline ferrites,[3] but it is likely that heat treatments producing appropriate microstructures could lead to materials with highly desirable properties.

The oxygen partial pressure plays an important role in the transformation behavior of cobalt ferrites since it affects the cation/anion stoichiometry. The ferrites were therefore transformed in two different oxygen environments: at about 500°C in the hot stage of the electron microscope (low P_{O_2}), and at 1230°C in air. The resulting microstructures have been observed in a 650kV electron microscope, and are discussed in this paper. Radiation damage during observation has been previously reported[4] but this effect does not induce precipitation as it does in silicon.[5]

2. EXPERIMENTAL

Specimens were obtained from the Airtron-Litton Industries in the form of small single crystals with a diameter of 2 to 3 mm. Analysis of the composition was done by first reducing the crystals to metal by heating them in hydrogen.* Then the Co/Fe ratio was determined with the standard chemical techniques. The composition of the crystals varied between $Co_{1.05}Fe_{1.05}O_4$ and $Co_{1.29}Fe_{1.72}O_4$. The as received crystals were annealed for about 50 hours at 900°C. According to the phase diagram,[6] Fig. 1, crystals of these compositions are then solid solutions. After air cooling, thin foils were prepared by chemical polishing described elsewhere.[4] The foils were examined in a 650 kV Hitachi transmission electron microscope. Some phase transformations have been followed in situ with the use of a hot stage specimen holder. Since the oxygen partial pressure greatly influences precipitation, the electron microscope atmosphere was analyzed at the specimen stage level with a Varian partial pressure gauge. The total pressure for the gases with a mass between 1 and 70 was measured to be about 5×10^{-6} Torr. Figure 2

---

* The chemical analyses have been performed by R. Clem, Chemistry Dept., Lawrence Radiation Laboratory, Berkeley, Calif. 94720

shows the readout of the gauge, from which the partial pressures can be calculated. Water vapor was the main gas phase which is common in unbaked vacuum systems. The partial pressures of the most important components have been listed in Fig. 2. Note that the atmosphere was not in equilibrium since it contained more free hydrogen than free oxygen. The reason is that low molecular weight gases are pumped less efficiently. It was expected that this atmosphere reacts to equilibrium at the specimen surface during the hot stage transformations, so that the excess hydrogen, together with the water vapor, determined the effective oxygen partial pressure. For most of the hot stage transformations the H_2/H_2O ratio was between 0.1 and 0.05. Such an atmosphere would, e.g. at 500°C, reduce CoO to metallic cobalt, but it would not reduce FeO. The composition of the microscope atmosphere did not remain constant over extended periods (days), so that in order to have comparable transformation data, the hot stage experiments were carried out when the prevailing atmospheres were comparable.

3. RESULTS

3.1 Transformations at reduced oxygen partial pressures: Hot stage experiments.

Foils of cobalt ferrite with a Co/Fe ratio between 0.54 and 0.76 were transformed in the hot stage of the microscope. In this composition interval no difference in morphology and nature of the transformations was observed. Most of the hot stage transformations were carried out at about 500°C. As was pointed out in the previous section, the microscope atmosphere is strongly reducing so that the foil continuously loses oxygen to its environment during the heating. The hot stage

experiments are for this reason dynamical so that different phase transformations may occur at different depths within the foil. For convenience, the events have been described in terms of an early, an intermediate, and a final stage.

3.1.1. The early stage

The early stage corresponds to the initial transformation interval in which rapid formation of small precipitates is observed. The observations were made on foils that had not been electron irradiated prior to transformation, though this precaution seemed to make no discernable difference.

The appearance of a foil transformed for 3 min. at about 500°C is shown in Fig. 3. Inspection of this image reveals that two different types of precipitates are present. The larger precipitates have been called Type 1, while the very small ones have been labeled Type 2. Stereomicroscopy techniques similar to those used previously for defect distributions in silicon[7] revealed that the precipitates are distributed in the foil as shown schematically in Fig. 4. The Type 1 precipitates are actually located very near to or at the top and the bottom surfaces of the foil. The Type 2 precipitates are located deeper inside the foil and are separated from the surface layer by an apparently precipitate free zone. A selected area diffraction pattern from the region of Fig. 3 is shown in Fig. 5a, together with its solution 5b. The precipitates have been identified by examination of numerous dark field images.* It turned out that the Type 1 precipitates were a mixture of cubic and hexagonal cobalt, while the very small Type 2 precipitates were shown to be a mixed sodium chloride type phase: (Co,Fe)O. These two precipitates are each shown

---

* For more detailed analyses, see ref. 8.

in dark field, in Fig. 6a and b. The metal precipitates imaged in Fig. 6a with a $10\bar{1}1$ hexagonal cobalt reflection are at this stage about 400Å in size, and are separated on the average about 1500Å. The cobalt-wüstite precipitates are imaged in Fig. 6b. The reflections that were isolated with the objective aperture are also shown in this figure. Note that although a matrix spinel reflection has been included, the background intensity is very low. This has been achieved by using a diffraction condition similar to the weak beam method used for resolving very closely spaced partial dislocations.[9] Note that the (Co,Fe)O precipitates are randomly distributed so that they do not give rise to the "satellites" to the matrix reflections as might result from a particular spatial precipitate arrangement. It was already shown in Fig. 6b that these satellites originate from the presence of cubic and hexagonal cobalt precipitates.

The orientation relationships between the precipitates and the matrix were simple; they are listed in Table 1.

TABLE I

type of precipitate	precipitate		matrix
cubic cobalt	(001)	//	(001)
	[100]	//	[100]
hexagonal cobalt	(0001)	//	(111)
	$[2\bar{1}\bar{1}0]$	//	[110]
cobalt-wüstite	(001)	//	(001)
	[100]	//	[100]

Since the oxygen sublattice parameter difference between the (Co,Fe)O precipitates and the spinel matrix is only 1.5%, these precipitates were likely to be completely coherent with the matrix. The oxygen sublattice should then be continuous in this two phase region.

It should be noted that in these early stages no significant decoration of dislocations by (Co,Fe)O was observed. This is illustrated in Fig. 7, which shows some dislocations that were present in the foil prior to the 3 min. heating at 500°C in the hot stage. Some of the end points of the dislocations or surface of the foil were, however, observed to be decorated by the surface cobalt metal precipitates.

3.1.2 The intermediate stage

A clear impression of the transformation events in the intermediate stage, has come from the observation of transforming wedged crystals. Figure 8 shows a time sequence of a foil being heated at 520°C. The elapsed time is indicated in the micrographs. Several observations can be made: The projected inner reaction zone, containing the cobalt-wüstite particles, is seen to shrink in size. A (Co,Fe)O particle marked with a black arrow near the receding boundary is seen to shrink in size, and eventually disappear completely. A (Co,Fe)O precipitate, marked with a white arrow, is, on the other hand, observed to increase in size somewhat. The size of the precipitates at this time was about 150Å, while the density was estimated as 2×10^{16} cm^{-3}. The larger particles, identified earlier as cobalt metal, are at the same time seen to grow, and in doing so they consume the surrounding matrix. This can be seen especially at the foil edges. The metal precipitates

remained attached to the matrix, and actually did change orientation somewhat so as to keep in physical contact with it. This motion, which is more or less determined by the local foil geometry and the nearness of other precipitates, slowly destroyed the original orientation relationship between the matrix and the metal precipitates.

3.1.3. The later stage

In the later stage the foil was near equilibrium with the surrounding atmosphere, and only grain growth (which appeared to be a slow process here) occurred. With the prevailing atmosphere and heating conditions, specimens consisted in this stage of a very highly cobalt rich metallic phase, and a spinel matrix which was consequently high in iron content (e.g. Fig. 9). The loss of the original orientation relationship can be deduced from the substructural features of the metallic phase, as may be inferred from a comparison between the features of the two metal grains marked A and B. The substructure of the metallic cobalt has been examined in somewhat more detail in Figs. 10 and 11. Figures 10 a and b show one grain consisting of alternating hexagonal and cubic cobalt, in an orientation relationship such that $(0001)_{hex}$ // $(111)_{cub}$, and $[2\bar{1}\bar{1}0]_{hex}$ // $[110]_{cub}$. Figure 11 shows another substructure in the cobalt grains that gives rise to long streaking in the diffraction patterns when the grain is exactly in the 110 orientation. Grains such as this one contain a high density of parallel faults, indicative of a single shear type transformation.

3.1.4. Hot stage transformations in less reducing atmospheres.

As has been mentioned in the experimental section, the composition of the microscope atmosphere did not remain constant over extended

periods. Whether or not free metal is thermodynamically possible at a given temperature depends critically on the excess hydrogen present. This excess was variable and, in fact, occasionally excess oxygen was found instead. The excess oxygen partial pressure was usually of the order of 10^{-7} to 10^{-8} Torr, and free metal should not be formed in that case. It was then to be expected that growth and coarsening of the wüstite type precipitates would just continue as the transformation proceeded. This was indeed the case, as is shown in Fig. 12 for a foil that was transformed for 10 min. at about 650°C in an effective oxygen partial pressure of about 2×10^{-8} Torr. It is interesting to note that the precipitates seem to periodically arrange.

3.2 Transformations in air.

Transformations in air at various temperatures confirmed the phase diagram, Fig. 1, in the composition interval that was studied. In order to be sure that the absence of precipitates was not due to a transformation proceeding from the free crystal surface, foils of cobalt ferrites were heated for up to 1 hr. in air at 500°C. Some thermal surface etching was in evidence, but no precipitates were found. Only the high temperature phase transformation was observed.

Crystals with a Co/Fe ratio of 0.76, so far the highest cobalt content available in the form of single crystals, were annealed for a series of times at 1230°C.

After 10 min. precipitates identified as (Co,Fe)O appeared. Some of these precipitates are shown in Fig. 13. The diffraction experiments revealed that these precipitates were in fact orthorhombic prisms, bounded by {100} planes. The size of these precipitates varied in the

same specimen; the largest coherent precipitate observed was 1200Å long.

Heterogeneously nucleated precipitates were also observed (Fig. 14) which show interface fringe contrast. In this figure the precipitate size decreases systematically upon going from A to B along the dislocation. After 60 min. of heating at 1230°C in air, large (Co,Fe)O precipitates were observed as shown in Fig. 15. The smallest precipitates which exhibited the type of interfaces contrast observed here, had a size of about 1500Å. Appropriate contrast experiments, suggested by the work of Gevers,[10] showed that the fringes at the interfaces were actually moiré fringes. A precipitate intersecting the foil edge, shown in Fig. 16, gave some more information about the details of the interface. The "bright spots" such as those marked 1 in this image have been resolved to be micropores. It is interesting to note that such micropores were never observed behind the (Co,Fe)O-matrix interface so that they are actually advancing together with the interface of the growing precipitate. The features encircled and labelled 2 in this image have been found to be interface dislocations not resolvably dissociated, with Burgers vectors in <110>.

Continued heating for up to six days at 1230°C in air did not lead to any different precipitate morphologies while at the same time no significant size increase was observed.

It is interesting to note that a small number of dislocations seemed invariably associated with these large, semi-coherent precipitates.

4. DISCUSSION

In order to explain the observed phase transformations it is necessary to consider the defect chemistry of oxidation, or reduction, of spinels, all e.g. by Schmaltzreid, Tretjakow, and Müller.[11-13] The main point

is that a reduction reaction can be written as:

$$2Co_O^{3+} + 4Fe_O^{3+} + 3V_O + CoFe_2O_4 \rightarrow 6Fe_O^{2+} + O_2(gas) \qquad (1)$$

where the subscript O refers to the cations on the octahedral interstitial positions, and V represents vacancies. Reduction thus actually results in the destruction of some ferrite crystal, while the excess cations of lower valence produced in this way are relocated in interstitial situ. Such a process increases the cation/anion ratio, constituting a deviation from stoichiometry. Large cation/anion non-stoichiometries, however, cannot be supported by most oxide crystals. Non-stoichiometric oxide crystals that were thought to be single phase actually contain, upon closer examination, extended structural defects that accommodate the cation or anion deficiencies. Prime examples of this are found in the oxides of transition metals of the titanium, vanadium and chromium groups.[14] Not always is the accommodation of non-stoichiometry as spectacular as in these shear type oxides, and in the case of cobalt ferrites an imposed increase in cation/anion ratio is simply accommodated by the precipitation of another near-stoichiometry phase with a higher cation to anion ratio: cobalt-wüstite. The reduction transformation reactions would be of the type:

$$3CoFe_2O_4 \rightarrow 2Fe_3O_4 + 3CoO + O_2\ (gas) \qquad (2)$$

A difficulty that is not reflected by this quasi-chemical approach is that reactions such as Eq. 1 and Eq. 2 cannot yield information on exactly how the oxygen leaves the crystal when a reduction transformation occurs. At any rate, a gradient of increasing ratio of metal/oxygen should exist from the bulk towards the surface of the oxide that is being

reduced. This deviation of stoichiometry was the main driving force of the transformation, since foils heated in air for up to 1 hour at 500°C failed to show any precipitates, while in the reducing atmosphere of the microscope the precipitation of (Co,Fe)O started almost instantaneously. Reduction (and consequently also oxidation) transformation should then always proceed in a layer-like fashion from the free crystal surface, where the local phase relation is largely determined by the local cation/anion ratio. This was reflected by the precipitate distribution found after brief hot stage transformations (section 3.1.1) and was observed during the dynamic intermediate stage (section 3.1.2) where the inner reaction zone was found to shrink. The time dependent cation/anion gradient can in principle be realized in two different ways: either by a metal ion excess, or by an oxygen ion deficiency. In the case of cation excess, the crystal should lose oxygen only at its very surface, and the excess cations of lower valence (Eq. 1) diffuse inward. If, on the other hand, the reduction creates an oxygen deficiency, then oxygen vacancies would be diffusing into the crystal from the surface. Without carefully measuring the reaction rates, it is not possible to decide which mechanism is operating, but since in cobalt ferrite (as in most oxides), the oxygen vacancy mobility is considerably lower than the cation mobility,[11] it seems more likely that the cation excess model applies. The transformation rates should then be controlled by the mobility of the faster moving cations, or maybe (but less likely) by the rate at which the oxygen desorption at the crystal surface occurs. As was found by Müller et al.,[11] the diffusion rate of these cations depends strongly on the vacancy

concentrations in the oxygen sublattice, and thus a function of the oxygen partial pressure.

The above considerations enable all the reduction transformation observations to be rationalized. For most of the hot stage experiments, the strongly reducing atmosphere of the microscope caused the ferrites to decompose into cobalt rich metal and an iron rich spinel, first at the surface of the foils, and later throughout the foil. The cobalt rich metal forms by a reaction such as [in a simplified way]:

$$3\ CoFe_2O_4 \rightarrow 3\ Co(s) + 2\ Fe_3O_4(s) + O_2\ (gas) \qquad (3)$$

Such a reaction is accompanied by a decrease in volume of about 25%. This significant volume change was reflected in the transforming foils by local changes in foil thickness, or even by the formation of holes around the growing metal particles. This was especially clear in Fig. 8. The analysis revealed that the cobalt actually consisted of a mixture of hexagonal and cubic cobalt such that $(0001/_{hex}$ // $(111)_{cubic}$, and $[2\bar{1}\bar{1}0]_{hex}$ // $[110]_{cub}$. This leads to the conclusion that the hexagonal cobalt forms from the cubic one, upon cooling of the specimen after transformation. The simultaneous presence of hexagonal and cubic cobalt is evidence that the metal grains contain at most 5% iron, since otherwise the hexagonal phase would not be formed.[15]

The presence of cobalt-wüstite phase is of a transient nature when the atmosphere is sufficiently reducing, so that these precipitates, after forming initially with very high density in an inner reaction zone, have to dissolve again. This was observed clearly in the intermediate transformation stage, as shown in Fig. 8. The coherent (Co,Fe)O precipitates near the boundary of the inner reaction zone were found to

dissolve, while some precipitates deeper inside this inner reaction region continued to grow.

The transformation leading to the precipitation of (Co,Fe)O, although initially proceeding very rapidly and giving high precipitate densities (3×10^{17} per cm.^{3}), was not spinodal, since the precipitates did form randomly, rather than in a modulated morphology. When the microscope atmosphere was less reducing, so that cobalt metal could not form, modulated (Co,Fe)O arrangements were observed after some coarsening had occurred. The modulated arrangement may not be due to spinodal decomposition, but rather develops after one initially random precipitate distribution, as a consequence of strain interactions during growth. Homogeneous transformations have also been found to occur in other spinel systems.[16] Similar phenomena have been found in metallic systems, and have been discussed by Ardell and Nicholson.[17]

The transformations in air at 1230°C are also reduction transformations since, according to the phase diagram, Fig. 1, the reaction is:

$$Co_{1.29}\,Fe_{1.79}O_4 \rightarrow 0.26(Co_{0.82}Fe_{0.18})O + 0.91\,Co_{1.18}\,Fe_{1.82}O_4 + 0.10\,O_2(gas) \qquad (4)$$

Oxygen non-stoichiometry, which is very likely to occur at this high transformation temperature, would slightly alter the amount of oxygen gas formed per mole of spinel that is transformed. Equation 4 shows that after complete transformation the (Co, Fe)O precipitates occupy about 7 vol.% of the crystal. Since the transformation reactions were of the same nature as in the hot stage experiments, certain similarities might be anticipated. The cation mobility could be estimated from the date of Schmaltzreid et al.[12,13] At 1230°C, the diffusion coefficient

of cobalt would be about 10^{-9} cm^2 sec^{-1}, so that after 100 sec, the mean diffusion distance of this cation would be about 10 micron. The samples that were transformed had a diameter of about 1 mm, so that, as was the case in the hot stage transformations, a reaction zone should develop from the specimen surface. Again, the transformation depended on the long range cation diffusion, since at all temperatures oxygen is the slower diffusing component. A confirmation of this may be seen in the observation of the two different types of (Co,Fe)O precipitate morphologies in identially treated material: viz., coherent orthorhombic prisms, Fig. 4, and precipitates decorating dislocations, Figs. 14,15. A tentative explanation of this "string of beads" morphology of Fig. 4 is as follows. The dislocation would end on the original free surface of the treated crystal. The lower left part of this dislocation would be further away from the free specimen surface, so that the precipitates that were formed there were smaller than the ones at A closer to the surface. Regardless of the location of the dislocation this observation evidenced that the wüstite-type precipitates nucleate heterogeneously at 1230°C in air.

After longer transformation in air at 1230°C, the interphase interface could be studied more clearly, and moiré fringes, interface dislocations, and micropores were found. At this stage the (Co,Fe)O precipitates were clearly semicoherent, and observations indicated that the precipitates lost coherency somewhere between 1200 and 1500Å.

Loss of coherency of growing precipitates has been discussed recently by Weatherly et al.[18,19] Several mechanisms have to be considered:

1. A punching mechanism in which one loop is emitted into the

matrix, when one loop is being formed at the interface.

2. Interface dislocations are supplied by sources in the matrix.

3. Interface dislocations are supplied by sources inside the precipitate.

4. Dislocations are nucleated at the interface by collapse of point defect aggregates.

These four possibilities are now examined in the framework of the experimental observations.

Although there are examples of systems in which punching occurs, see e.g. Eikum and Thomas,[20] mechanism 1 did not seem to be operating in the precipitation of (Co,Fe)O from cobalt ferrite. The dislocation density that was observed in the neighborhood of the large precipitates was too low to be in agreement with the punching model. Also, a minimum amount of misfit, about 4%, between the lattice parameters of the precipitate and the matrix, appears to be necessary.[18] In the present cases, this misfit is only 1.5%.

Since the dislocation density in the crystal was low at the start of the transformation, it is highly unlikely that the misfit dislocations would be supplied from the matrix. For this reason, mechanism 2 was discarded.

Mechanism 3 requires the nucleation of a dislocation loop inside the precipitate. No defects, such as stacking faults, were found in the (Co,Fe)O precipitates when they were fully coherent. Although the spontaneous nucleation of dislocations in the perfect precipitates is possible,[21] it is a high energy event.

The present observations indicated that the mechanism involving

collapse of the point defects at the precipitate surface was the one by which the precipitate lost coherency. Vacancies accumulating near the interface may eventually collapse into prismatic loops. The loops could expand by climb along the precipitate surface thus reducing the interstitial type stress field that surrounded the coherent particle. Once a loop was nucleated, the creation of more interface dislocations would follow in a more or less catastrophic way, as was suggested by Weatherly and Nicholson.[18] Occasionally, a dislocation might be produced, by plastic deformation of the precipitate surroundings, as was suggested by the observation of the few dislocations that invariably seem to be associated with semi-coherent precipitates.

The micropores that developed must have migrated along with the interface, since no pores were ever found behind the matrix-precipitate interface. It is very doubtful that they would form upon cooling of the sample from the transformation temperature, since the cooling rates were several hundred degrees per minute.

The formation of micropores during the transformation can only be explained by a mechanism which involves the transport of oxygen vacancies. A tentative mechanism of their formation would be as follows:

It was already pointed out that the formation of the cobalt-wüstite precipitates is controlled by the long range cation diffusion from the free surface of the crystal. At 1230°C, however, this is a simplification, since the mobility of the oxygen vacancies must be sufficient to participate, at least to a small extent, in the precipitation phenomenon. Part of the gradient in cation/anion ration must then be realized by the inward diffusion of oxygen vacancies. These oxygen

vacancies, V_O, are created at the surface of the heated crystal by reactions such as

$$4\ Fe^{3+} + 2\ O^{--} = O_2(gas) + 2\ V_{Ox} + 4\ Fe^{2+}\ \ldots \qquad (14)$$

Both the oxygen vacancies and the divalent cations diffuse toward the precipitate, where the phase transformation is continuing. The growing cobalt-wüstite precipitate consumes a large amount of divalent cations, but it cannot incorporate the oxygen vacancies. As the precipitate increases in size, an excess of oxygen vacancies would then build up near the spinel - (Co,Fe)O interface. Since these oxides cannot support large deviations from stoichiometry, the oxygen vacancies will have to cluster, first as vacancy loops, and later as actual voids, as in the mechanism by which the precipitates lose coherency. The climb of the vacancy loops is limited by the requirement that they have to remain at the interface in order to accommodate the lattice parameter differences between matrix and precipitate. The dislocations and the micropores then act as effective oxygen vacancy sinks, allowing further participation of oxygen in the transformation. Once a free surface is present internally, a reaction such as expressed by Eq. 4 can take place. This would on the one hand increase the pore size somewhat, but on the other hand, it would fill the pore with oxygen gas. When the equilibrium oxygen pressure has been reached, this reaction must cease. The presence of oxygen gas in the micropores might be inferred from their nearly spherical shape. The partial pressure of the oxygen gas should be sufficient to overcome the tendency of the pores to be bounded by low index crystallographic planes. This tendency is due to the anisotropy of the surface

energy. A rough estimate of the pore volume showed that they took up about 0.3% of the volume of the precipitate. This was certainly not sufficient to compensate for the overall 2.5% decrease in volume that accompanied the transformation but it is direct evidence for the participation of oxygen ions in the phase transformation.

A characteristic of all the reduction transformations that have been reported here is that they all develop as reaction zones proceeding from the free crystal surface.

This layer morphology during oxidation and reduction transformations poses so many manufacturing problems that the properties of practical Oxides are usually controlled by variation of grain size, porosity, or by addition of inert inclusions.[3] Also, transformation strains are not easily accommodated, since most ceramic oxides remain intrinsically brittle up to high temperatures, so that precipitation often causes cracking. In cobalt ferrites, however, our work has shown that a two phase structure can be produced by a reduction transformation without the nucleation of cracks. The practical usefulness of this reduction transformation is necessarily limited to thin film applications due to its layering nature, but this is not really a great drawback, since thin films are used extensively in microelectronics. The most interesting transformations, from a practical point of view, are those in the strongly reducing atmospheres, since it has been found that a density of small (Co, Fe)O precipitates as high as 3×10^{17} per cm^3 can be produced. Such a substructure in cobalt ferrite may well produce a magnetic ceramic with an extremely high coercive force. The advantage of such a reduction transformation is that it can be used over a wider composition range

than the spinodal decompositon reaction that has been observed in some cobalt ferrites.[22]

ACKNOWLEDGEMENTS

The authors wish to acknowledge many useful discussions with Dr. P. Okamoto. The partial pressure gauge was kindly provided by Dr. D. Olander. D. Jurica and M. Robson are thanked for their technical assistance. This work was done under the auspices of the U.S. Atomic Energy Commission through the Inorganic Materials Research Division of the Lawrence Radiation Laboratory.

REFERENCES

1. E. W. Gorter, Philips Res. Rep. 9, 295 (1954).
2. E. C. Snelling, Proc. British Ceram. Soc. 2, 151 (1964).
3. A. Broesse van Groenau, P. F. Bongers, and A. L. Stuyts, Mat. Sci. and Eng. 3, 317 (1968).
4. L. C. De Jonghe and G. Thomas, J. Appl. Phys. 41, 4884 (1970).
5. E. Nes, Ph. D. Thesis, U. C. Berkeley, UCRL-19608, August 1970.
6. J. Robin, Ann. Chim. 10, 393 (1955).
7. E. Levine, G. Thomas and J. Washburn, J. Appl. Phys. 38, 81 (1967).
8. L. C. De Jonghe, Ph. D. Thesis, U. C. Berkeley, UCRL-20369, Dec. 1970.
9. D. J. H. Cockayne, I. L. F. Ray and M. J. Whelan, Phil. Mag. 20, 1265 (1969).
10. R. Gevers, Phil. Mag. 7, 1681 (1962).
11. W. Muller and H. Schmaltzreid, Ber. Bunsenges, Physik. Chem. 68, 270 (1964).
12. H. Schmaltzreid, Progress in Solid State Chemistry 2, Pergamon Press, 1965.
13. H. Schmaltzreid and J. D. Tretjakow, Ber. Bunsenges. Physik. Chem. 70, 180 (1966).
14. A. Magneli, The Chemistry of Extended Defects in Non-metallic Solids, ed. L. Eyring and M. O'Keeffe, North-Holland Pub. Co., Amsterdam, 1970.
15. M. Hansen, Constitution of Binary Alloys, McGraw-Hill, N.Y., 1958, p. 472.

16. M. E. Fine, The Chemistry of Extended Defects in Non-metallic Solids, ed. L. Eyring and M. O'Keeffe, North-Holland Publ. Co., Amsterdam, 1970, p. 575.

17. A. J. Ardell and R. B. Nicholson, Acta Met. 14, 1295 (1966), and J. Phys. Chem. Solids 27, 1793 (1966).

18. G. C. Weatherly and R. B. Nicholson, Phil. Mag. 17, 801 (1968).

19. G. C. Weatherly, Phil. Mag. 17, 791 (1968).

20. A. Eikum and G. Thomas, Acta Met. 12, 537 (1964).

21. J. J. Hren and G. Thomas, Trans AIME 227, 308 (1963).

22. M. Takahashi and M. Fine, Am. Ceram. Soc., West Coast Annual Regional Meeting, October 1970.

FIGURE CAPTIONS

Fig. 1. Phase diagram at 1 atm of air.

Fig. 2. Partial pressure gauge readout. The partial pressures of the most important gases in the electron microscope are listed.

Fig. 3. Two types of precipitates are observed in a foil of cobalt ferrite, after heating for 3 min at 500°C, in the electron microscope.

Fig. 4. Location of the precipitates in a foil heated for 3 min at 500°C, in the hot stage of the electron microscope.

Fig. 5. a) Diffraction pattern of area shown in Fig. 31.
b) Solution to Fig. 5a.

Fig. 6. a,b) Dark field images of indicated reflections. The very small precipitates (~30-40Å) are (Co,Fe)O, the larger ones are a mixture of hexagonal and cubic cobalt. Note that the (Co,Fe)O precipitates randomly.

Fig. 7. No preferential decoration of dislocations by the (Co,Fe)O phase is observed. This indicates that the nucleation of this phase is homogeneous.

Fig. 8. Time sequence showing how the reaction proceeds in a wedge shaped foil. The elapsed time is indicated. Note the shrinking of the inner reaction zone. Note also how the matrix is consumed around the growing cobalt particles, especially at the foil edge.

Fig. 9. Cobalt grains in late transformation stage show clear substructure.

Fig. 10 a,b) Analysis of a cobalt grain shows that the substructure is due to the presence of cubic and hexagonal cobalt.

Fig. 11. Cobalt grain showing nearly periodic twinning or faulting. The substructure acts as a phase grating, giving rise to a succession of very closely spaced diffraction spots.

Fig. 12. Modulated (Co,Fe)O precipitate arrangements can be found after transformation, if the transformation to metal + spinel does not occur. The modulation does not originate in spinodal decomposition.

Fig. 13. (Co,Fe)O precipitates as small square prisms, bounded by {100} planes, when cobalt ferrite is heated for 10 min at 1230°C in air. Note the particular shape of the line of no contrast when g = 440.

Fig. 14. Decoration of dislocation by (Co,Fe)O shows that the transformation is heterogeneous at 1230°C in air. Note that there is still evidence of strain.

Fig. 15. Large precipitates of (Co,Fe)O in cobalt ferrite after heating for 60 min at 1230°C in air. Note the presence of a few dislocations, and the peculiar interface contrast.

Fig. 16. Large (Co,Fe)O precipitate at the foil edge. The geometry is drawn in perspective. The foil surfaces intersect the precipitate in the shaded areas. "Bright spots" at the interface are marked 1. Possible interface dislocations are marked 2.

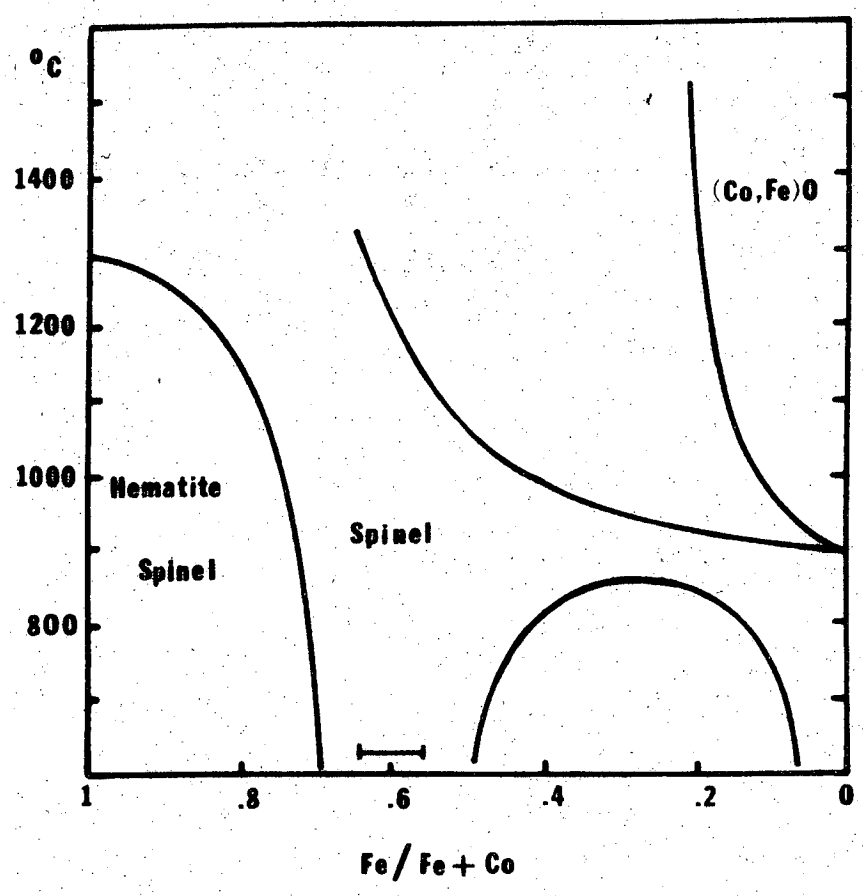

XBL 7010-6692

Figure 1.

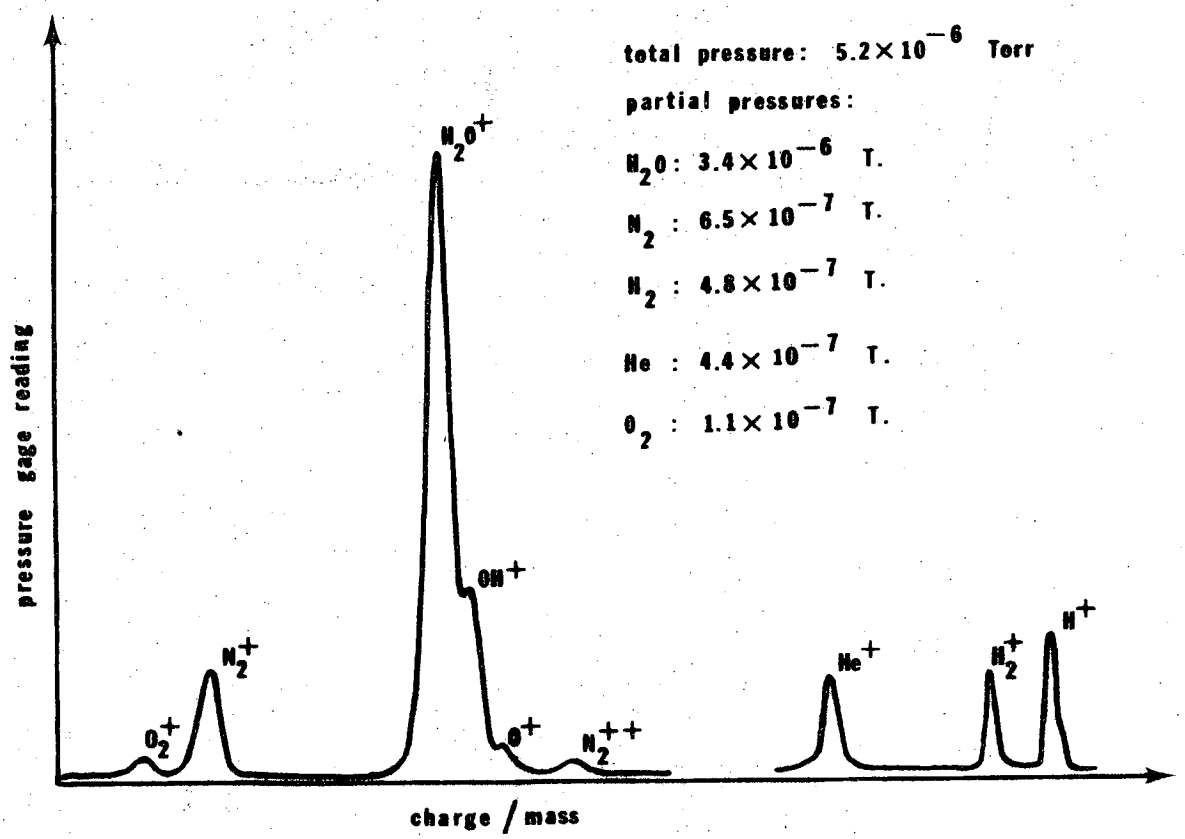

XBL 7010-6691

Figure 2.

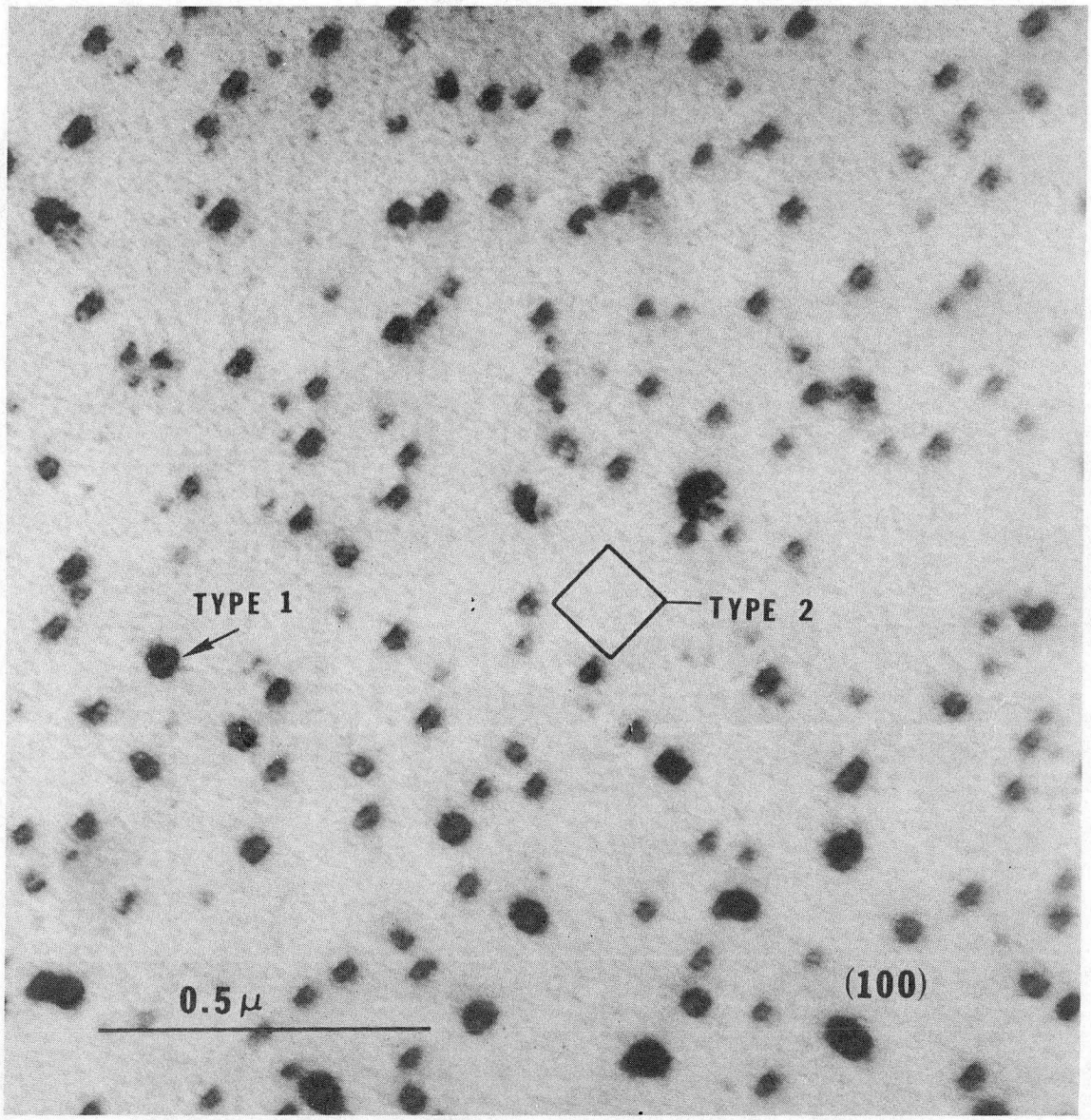

XBB 709-3940

Figure 3.

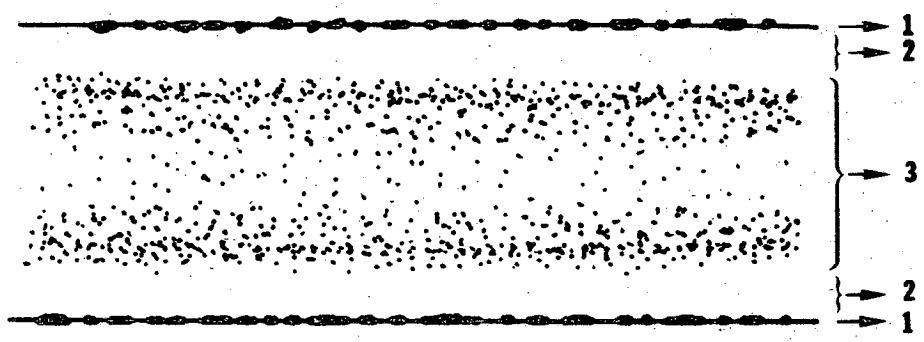

1- type 1 precipitates in surface layer

2- precipitate free region

3- inner reaction zone with type 2 precipitates

XBL 709-6569

Figure 4.

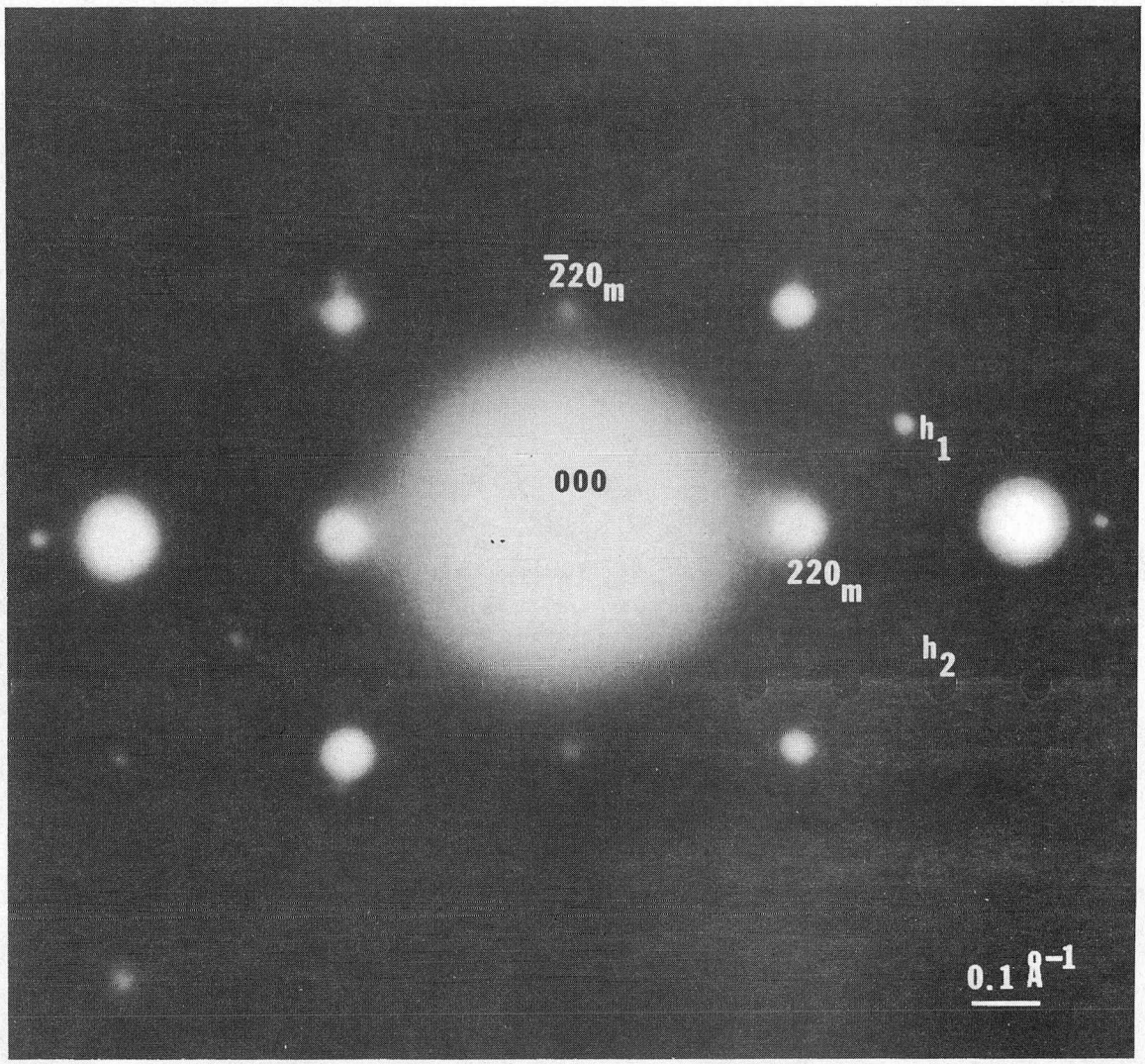

XBB 709-4015

Figure 5a

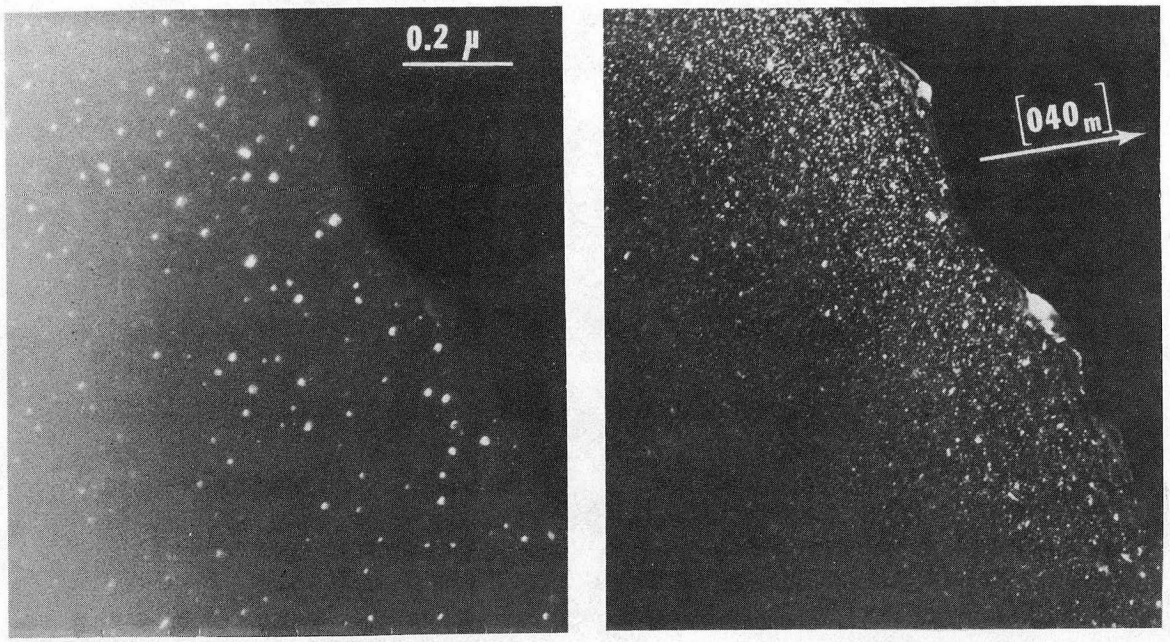

a DF h_2 b

(100)

XBB 709-4342

Figure 6a,b

XBB 709-3934

Figure 7

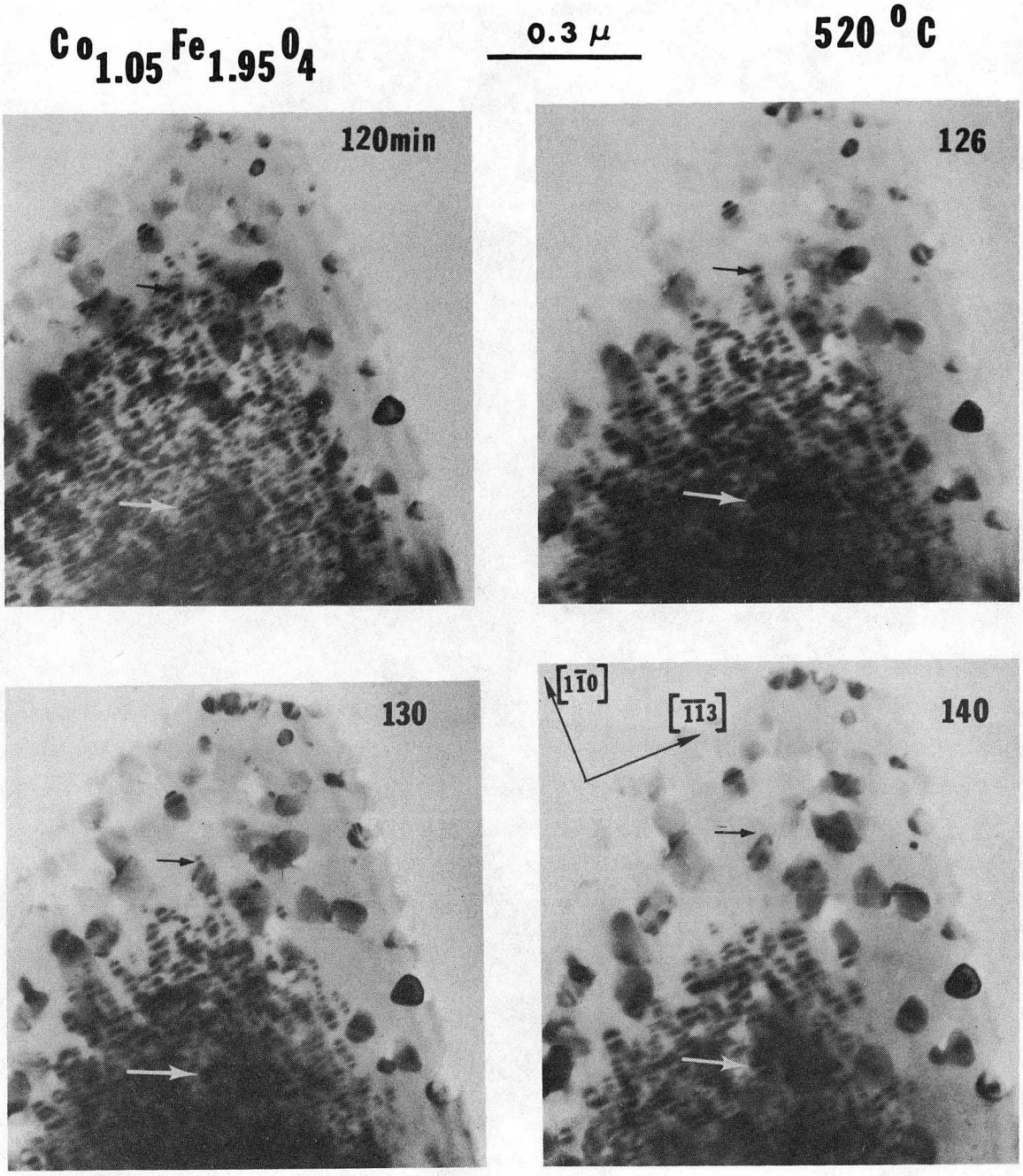

XBB 709-4012

Figure 8

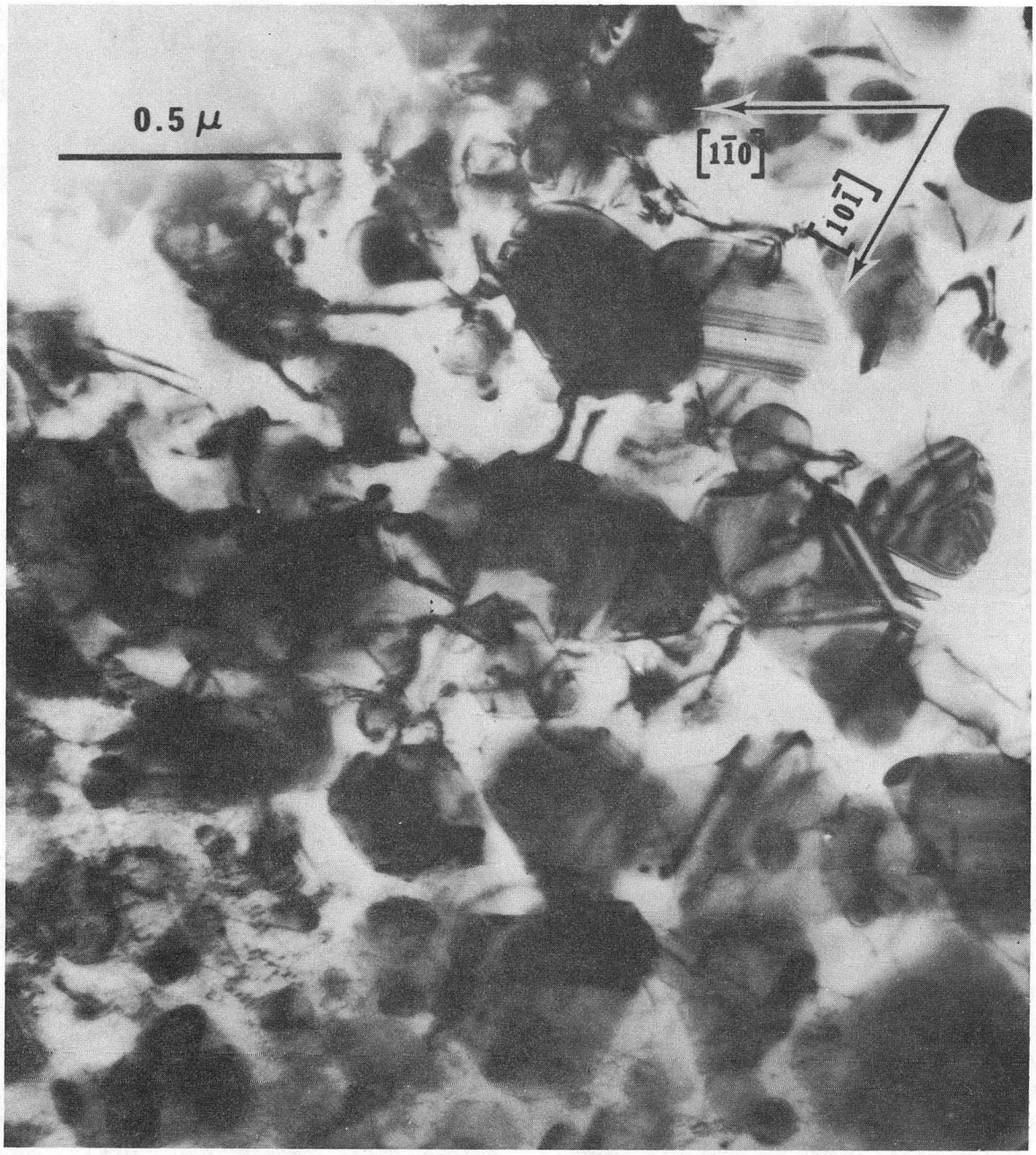

XBB 709-4016

Figure 9

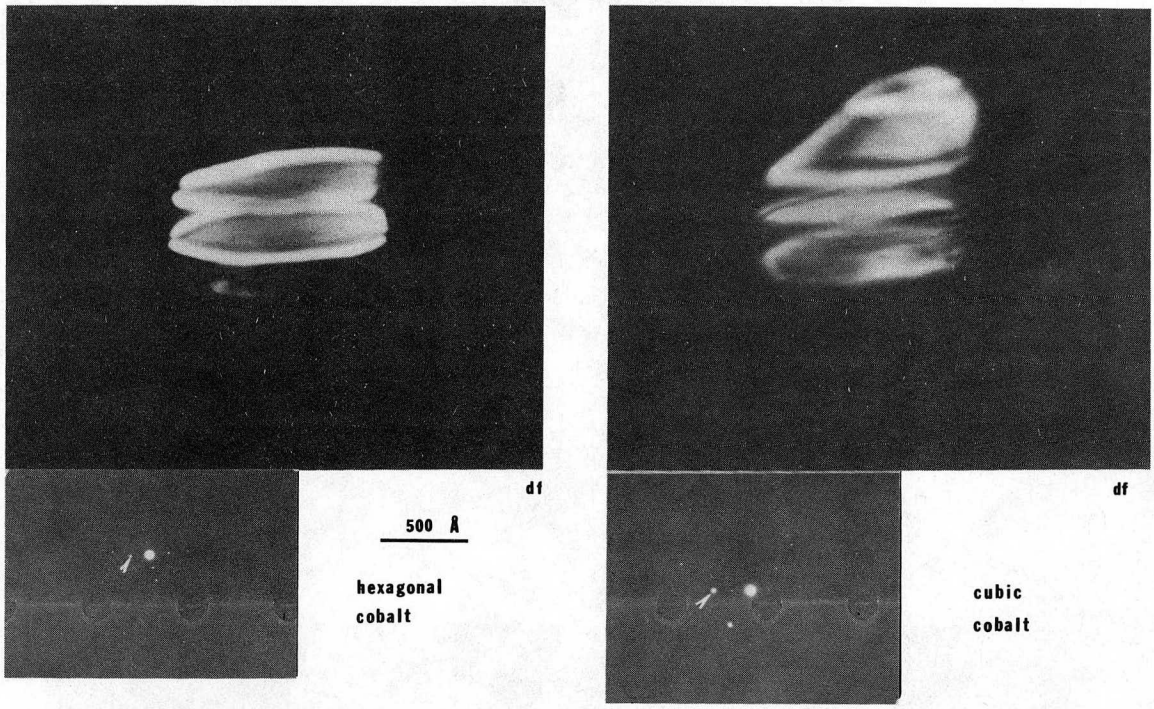

XBB 709-3936

Figure 10a,b

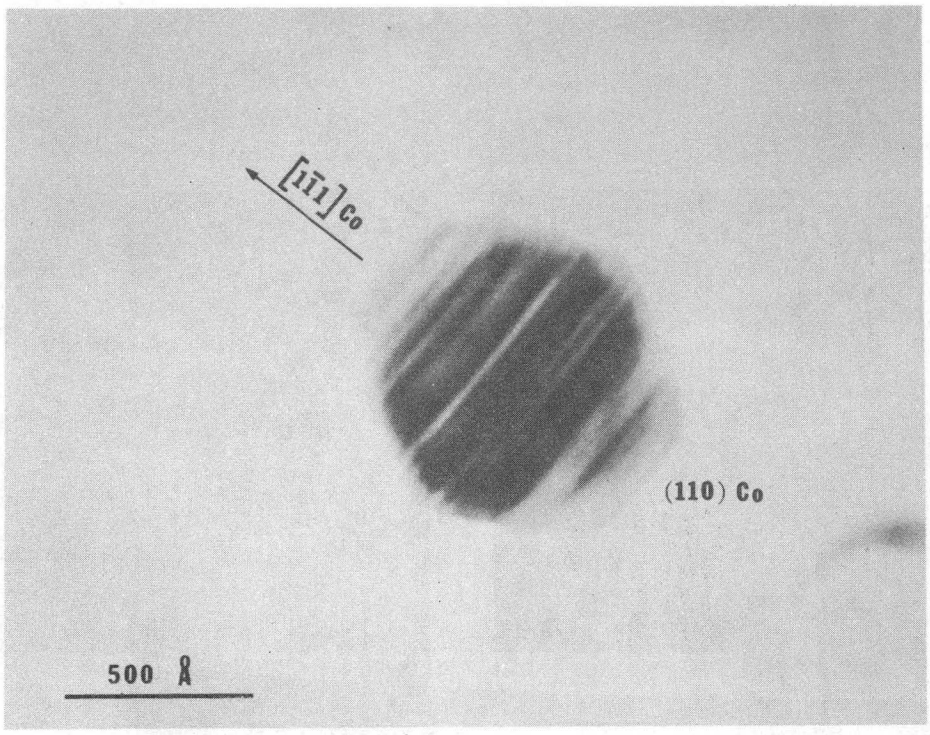

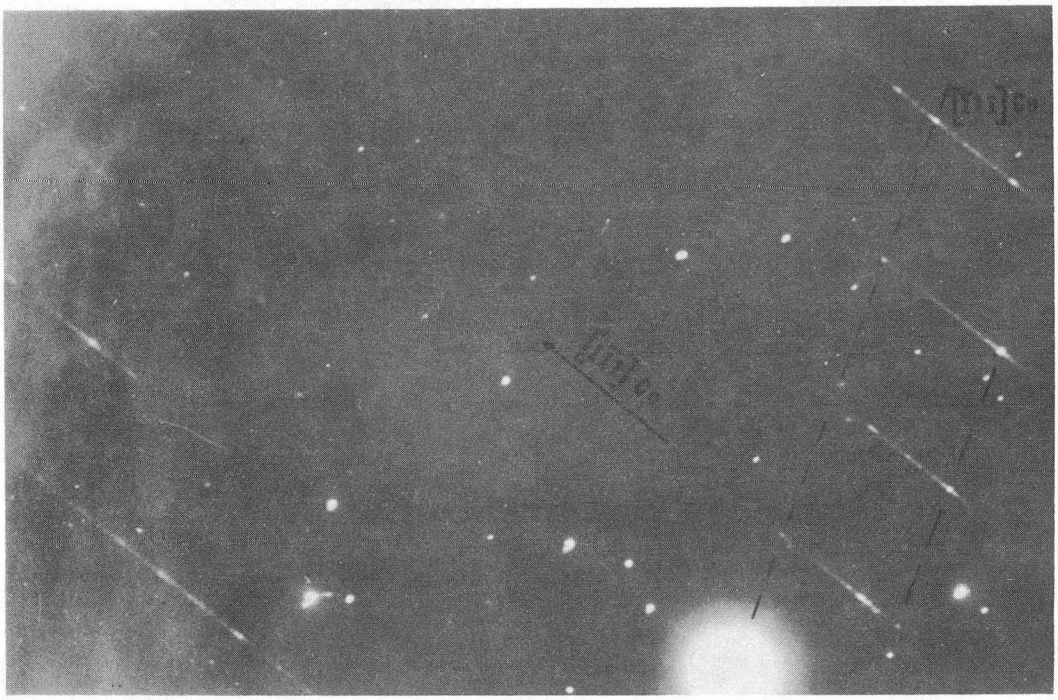

XBB 7011-5242

Figure 11

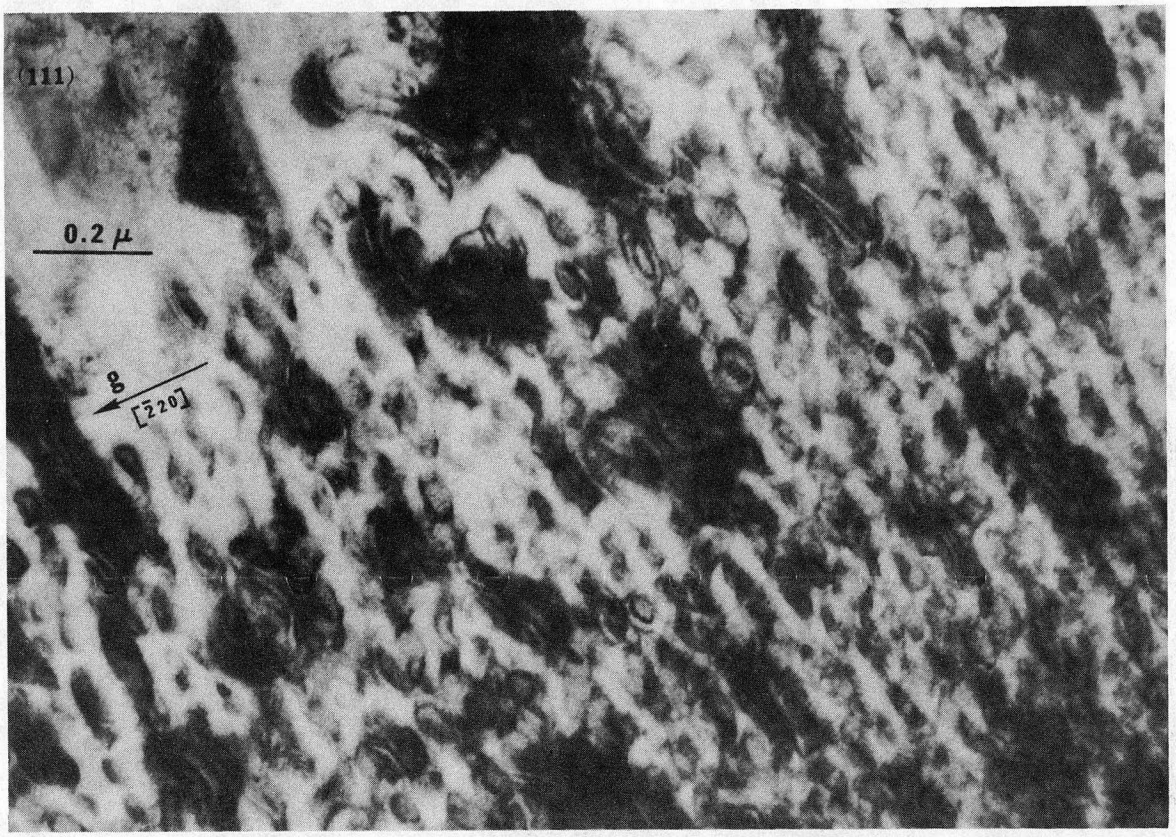

XBB 7010-4498

Figure 12

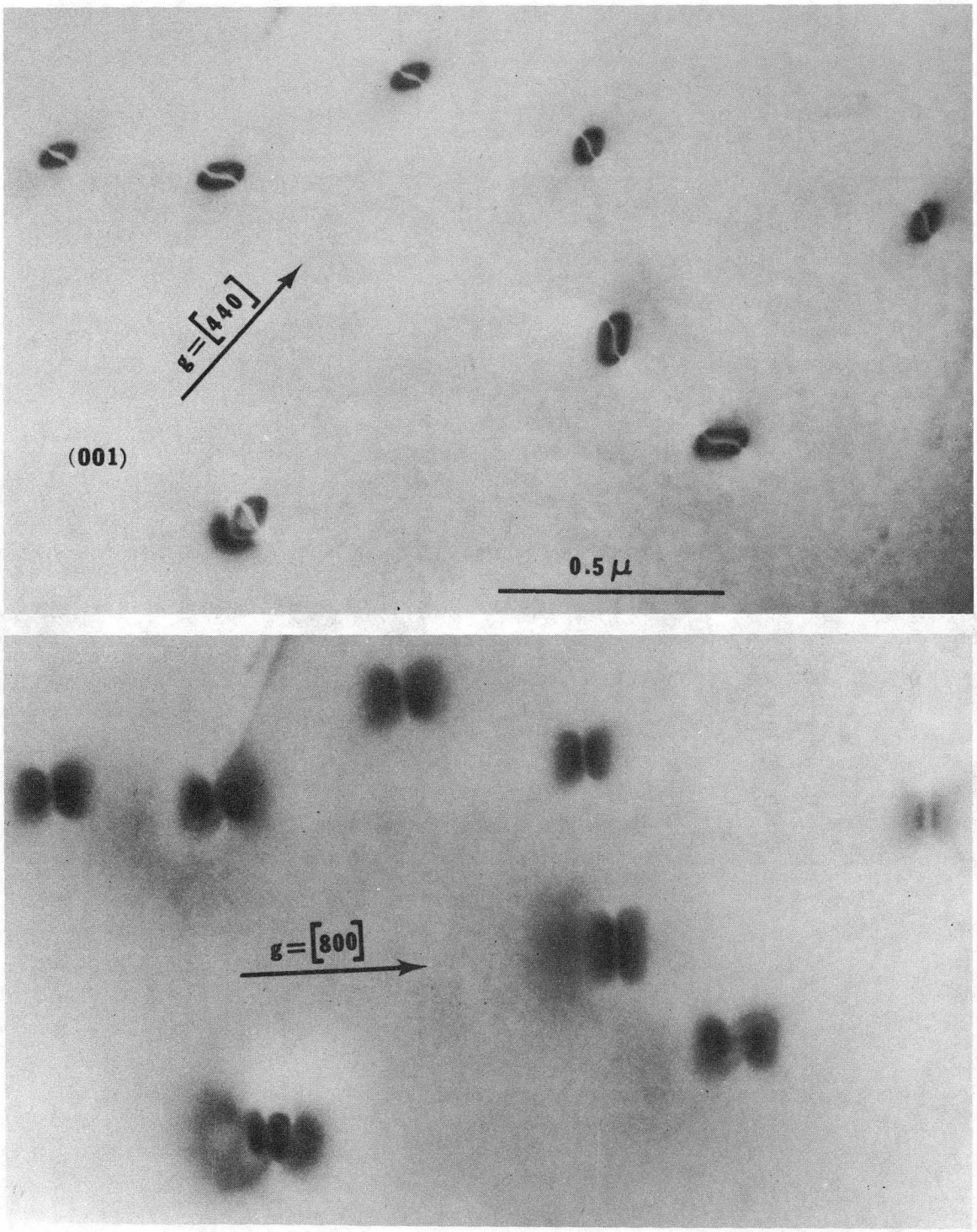

XBB 7010-4577

Figure 13

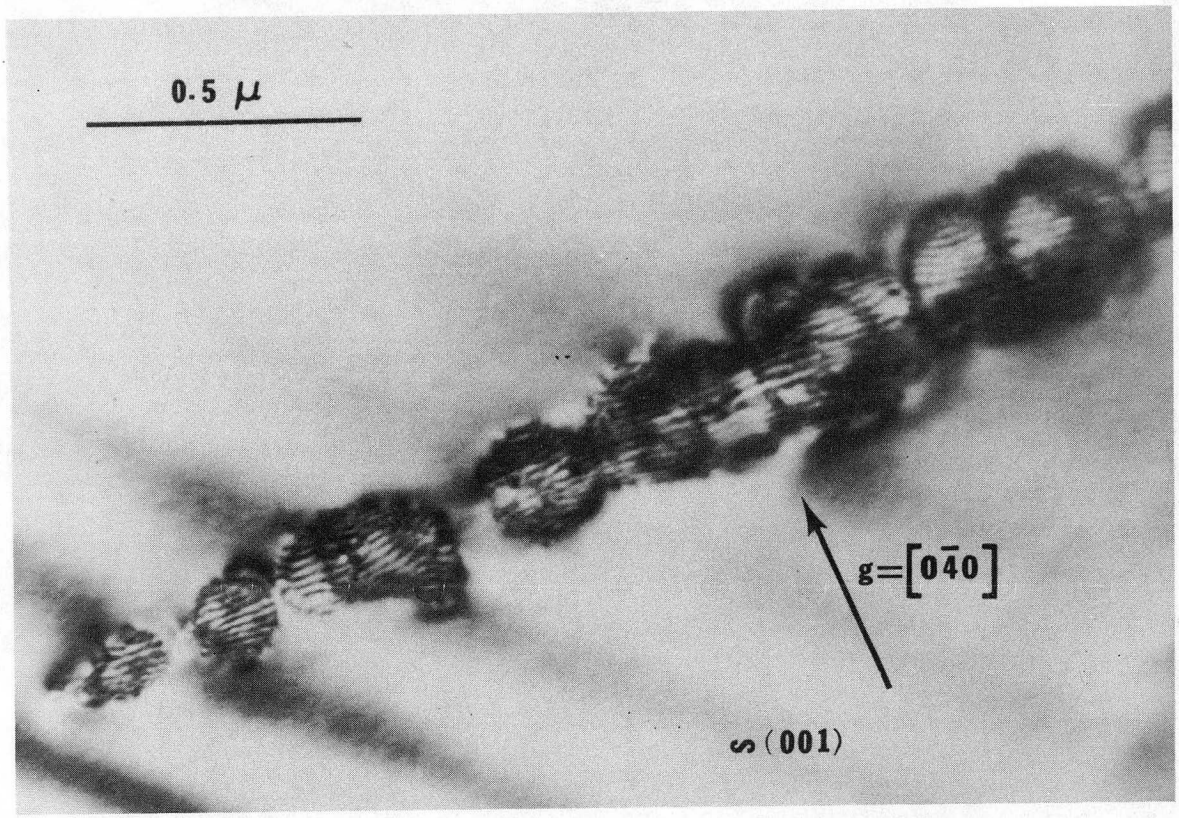

XBB 7010-4578

Figure 14

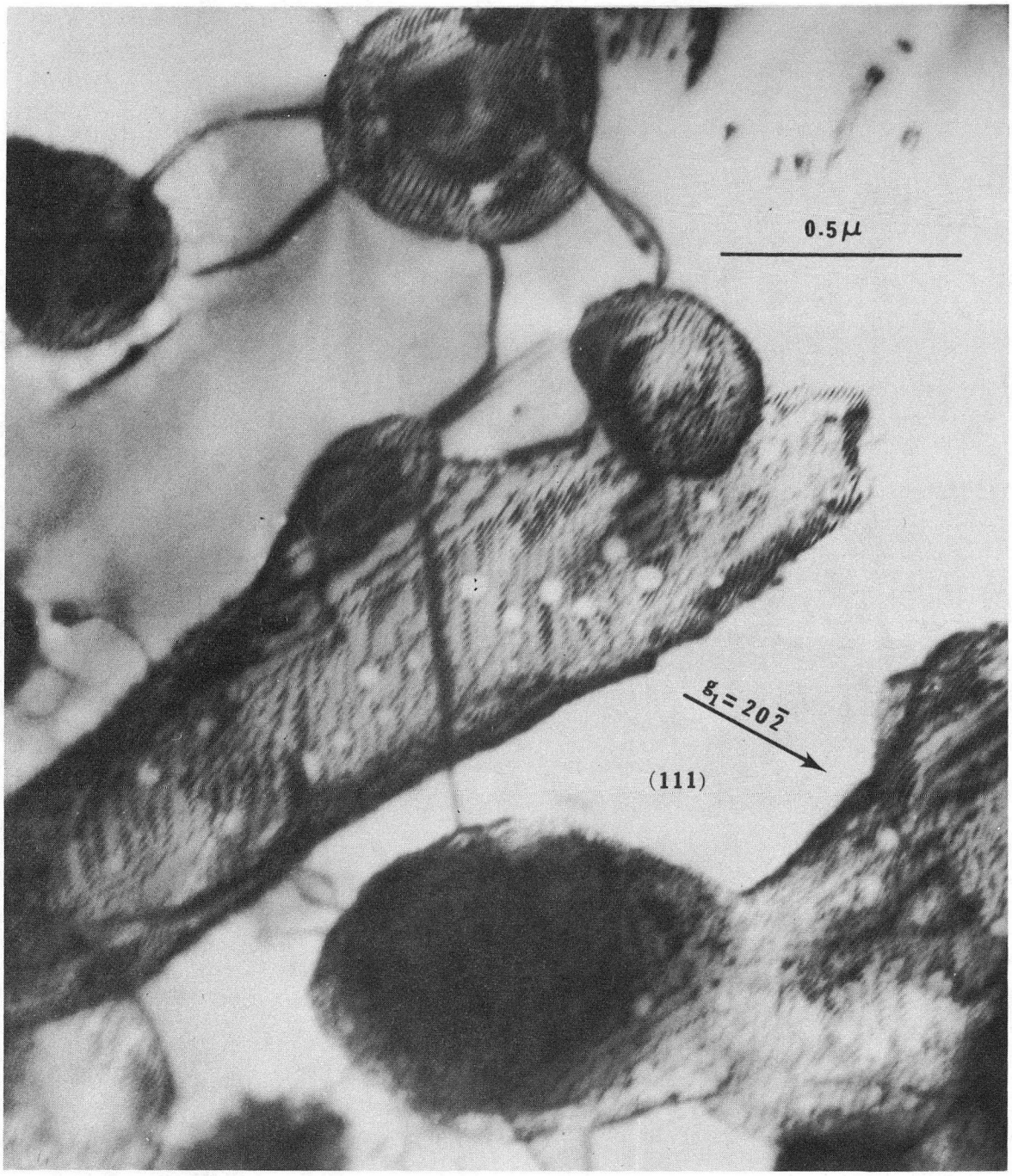

XBB 709-4350

Figure 15

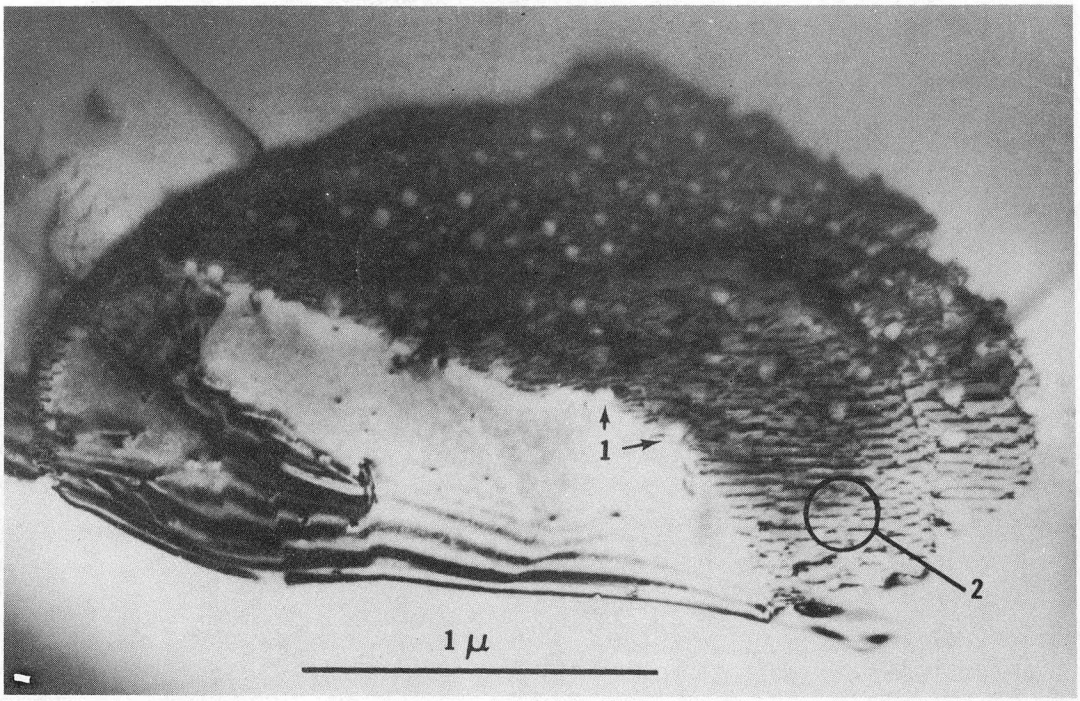

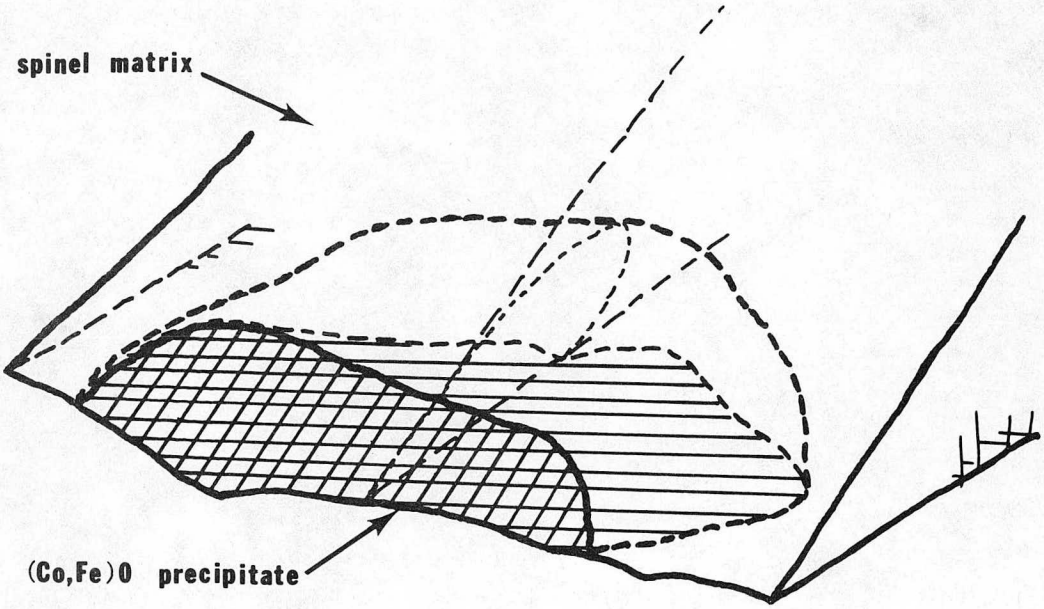

XBB 709-4344

Figure 16

LEGAL NOTICE

This report was prepared as an account of work sponsored by the United States Government. Neither the United States nor the United States Atomic Energy Commission, nor any of their employees, nor any of their contractors, subcontractors, or their employees, makes any warranty, express or implied, or assumes any legal liability or responsibility for the accuracy, completeness or usefulness of any information, apparatus, product or process disclosed, or represents that its use would not infringe privately owned rights.

TECHNICAL INFORMATION DIVISION
LAWRENCE RADIATION LABORATORY
UNIVERSITY OF CALIFORNIA
BERKELEY, CALIFORNIA 94720